Fracture Mechanics of Concrete and Concrete Structures -
Assessment, Durability, Monitoring and Retrofitting of Concrete Structures- B. H. Oh, et al. (eds)

Interfacial bond-slip behavior between CFRP plates and concrete

Sung-Nam Hong,
Sungkyunkwan University, Suwon, Korea

Jae-Joong Shim
Sungkyunkwan University, Suwon, Korea

Dong-Suk Yang
Korea Infrastructure Safety and Technology Corporation, Goyang, Korea

Taewan Kim
Sungkyunkwan University, Suwon, Korea

Sun-Kyu Park
Sungkyunkwan University, Suwon, Korea

ABSTRACT: This paper first investigates the interfacial bond behaviour in the shear test for CFRP laminates bonded to concrete. Two concrete compressive strengths are considered. For each concrete, the effective bond length is estimated using a linear regression analysis; the maximum bond stresses and slips at different load levels are calculated from measured strains in the CFRP laminates. Also, a simple bond–slip model for the CFRP/concrete joints, developed from the shear tests, is proposed and used in a nonlinear finite element analysis of beams strengthened in flexure with bonded CFRPs. Comparisons are made between the analytical and experimental results for the CFRP-strengthened beams. Very good agreement between the numerical predictions and test values is obtained.
Key words: CFRPs, debonding, ductility, finite element analysis, flexural tests, shear tests.

1 INTRODUCTION

The strengthening of reinforced concrete structures with advanced fibre reinforced polymer (FRP) composites has become very popular in the past few years. The use of FRPs for upgrading and strengthening civil concrete infrastructure has been accepted only in a gradual manner. In the past, FRP materials were used primarily in the aerospace and defence industries rather than in civil engineering construction, mainly due to the prohibitively high cost of the raw materials and manufacturing processes. However, due to both the need for maintaining and upgrading essential infrastructure in all parts of the world and the well-known advantages of FRP composites, including both good corrosion resistance and ease for site handling due to their light weight, the use of FRPs in structural rehabilitation has increased considerably. The continuous reduction in the material costs of FRP composites is also contributing to their popularity.

It has been reported that, when tested to failure, most concrete structures strengthened in flexure using composite materials exhibit debonding modes of failure [2, 9, 13]. Also, because of the complex interfacial shear behaviour between bonded FRPs and concrete, a theoretical approach towards the analysis of debonding failures is quite complicated [5, 11]. Furthermore, given the brittle nature of debonding failures in FRP-strengthened structures [18], the mechanisms regarding bond performance need to be clearly understood in order to establish safe strengthening designs [19].

This paper first investigates the interfacial bond behaviour in the shear test for CFRP laminates bonded to concrete. Shear tests have been performed for two concrete compressive strengths (21MPa, 28MPa) and various bonding lengths (100mm, 150mm, 200mm, 250mm) as variables in the experimental program. The effective bond length for each concrete compressive strength is estimated using a linear regression analysis; the maximum bond stresses and slips at different load levels are calculated from the measured strains in the bonded CFRP laminates. A simple bond–slip model for the CFRP laminates in the shear test is proposed, and then applied in a nonlinear finite element analysis of CFRP-laminated concrete beams tested in flexure. The analysis is verified against the flexural tests. Also, the ductility (the ratio of the deflection at the yield load to the deflection at debonding failure) is evaluated for each of the tested beams.

2 SHEAR TESTS FOR CFRP LAMINATES BONDED TO CONCRETE

2.1 *Materials and specimens*

A total of eight specimens with CFRP laminates bonded to concrete prisms were tested in shear (Figs. 1 and 2). The specimen size was a rectangular section of dimensions 100mm × 100mm × 300mm (width × height × length). In order to apply the loading force, concrete blocks having reinforcing bars were inserted into a tensile loading frame. One of the blocks had only the bonded CFRP laminates, while the other consisted of a similarly bonded CFRP laminate with an additional CFRP sheet wrap to prevent debonding on this block. Strains and slips were not measured for this second block.

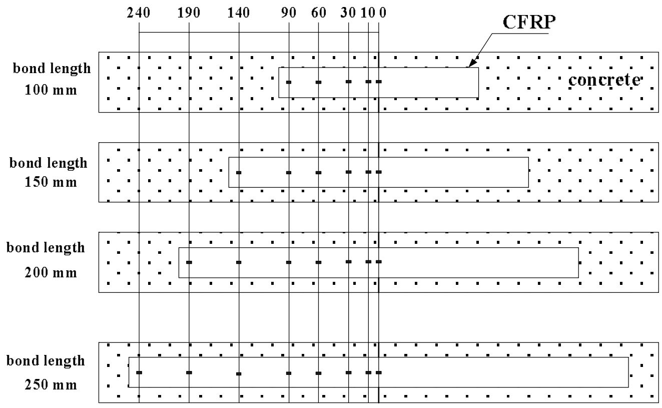

Figure 1. Locations of strain gauges (units: mm).

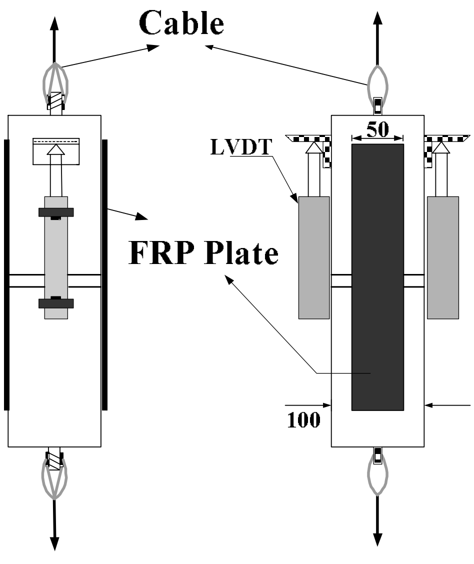

Figure 2. Loading of specimens (units: mm).

The material properties of the CFRP laminates are provided in Table 1, while the CFRP sheet and resin material properties are given in Table 2. As variables for the shear tests for the CFRP/concrete joints, various bonding lengths for the CFRP laminates (100mm, 150mm, 200mm, 250mm) and concrete compressive strengths (21MPa, 28MPa) have been selected

Table 1. Material properties of CFRP laminate.

	Tensile Strength (MPa)	Modulus of elasticity (MPa)	Remarks
CFRP laminate	2,350	1.73×10^5	Width 50mm Thickness: 1.3mm
Epoxy resin	33.5	1,500 ~ 3,500	Bond strength: 4.3MPa

Table 2. Material properties of CFRP sheet.

	Weight (g/m^2)	Width (mm)	Thickness (mm)	Tensile Strength (MPa)	Modulus of elasticity (MPa)
SK-N300	300	500	0.167	3,550	2.35×10^5
SK-resin	-	-	-	30.0	1.50×10^3

The specific details of the specimens are given in Table 3. As can be seen here, the thickness of the resin is about 3mm, and the width of CFRP laminate in the shear tests is 50mm.

Table 3. Details of specimens in shear tests.

Specimens	Epoxy Thickness (mm)	Bond Width (mm)	Concrete Compressive Strength (MPa)	Bond Length (mm)	Remarks
D21-10				100	
D21-15			21	150	
D21-20				200	
D21-25	3.0	50.0		250	
D28-10				100	
D28-15			28	150	
D28-20				200	
D28-25				250	

2.2 *Loading equipment and arrangement of strain gauge*

In order to measure the strains in the CFRP laminates during loading, strain gauges have been bonded to the CFRP laminates as shown in Figure. 1. The CFRP laminates were bonded on both sides of the specimens so that the mean values of the strains could be obtained. The loading was increased monotonically. Because the bond strength was very small, the rate of loading was kept as low as possible. The data were automatically collected by a computer data acquisition system.

As shown in Figure. 2, a rebar has been inserted in both sides of the specimen for the tensile loading in a manner to minimize eccentric loading. In addition, an LVDT was attached to each side of the specimen in order to measure slip during loading.

3 RESULTS AND DISCUSSION OF SHEAR TESTS

3.1 *Test results*

The results of the shear tests of eight specimens having bond lengths of 100mm, 150mm, 200mm, and 250mm are summarized in Table 4. These shear test results indicate that, as expected, the ultimate load increases as the bond length increases. In this table, the effective bond length (the bond length beyond which the ultimate load no longer increases) was estimated using the linear regression analysis shown in Figure. 3. From these results it can be concluded that the effective bond length can be taken in the range of about 196~204mm. Regardless of the concrete compressive strength, the average bond stress decreases until the effective bond length is reached, and the average bond stress becomes constant when the bond length is greater than the effective bond length.

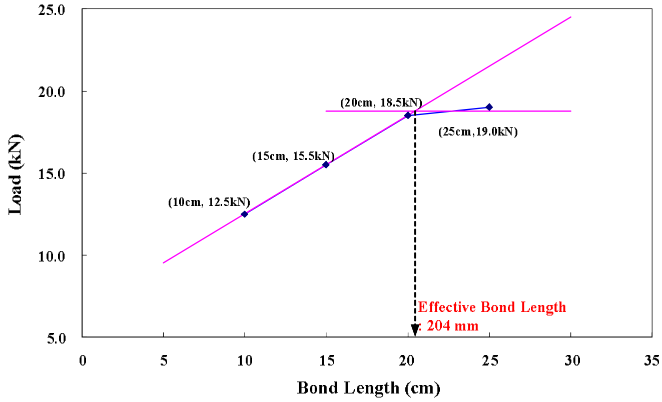

(a) D21 series

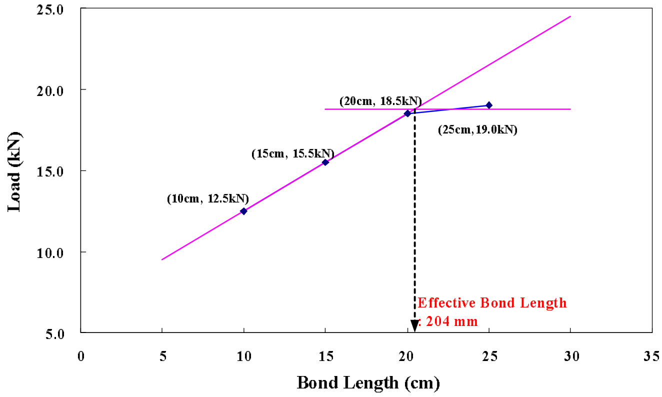

(b) D28 series

Figure 3. Estimation of effective bond length.

3.2 *Relation between loads and strains in CFRP laminates*

In order to measure the strain gradients along the bonded lengths of the CFRP laminates, strain gauges have been placed as shown in Figure. 1. The failure mode for each specimen was due to debonding of the CFRP laminates, as shown in Figure. 4. The load–CFRP strain curves at the various locations are shown in Figure. 5 for each specimen. As can be seen in Figure. 5, at a given load level the maximum strain occurs at the beginning of the bonded joint (gauge at 10mm). In the initial loading stages the load–strain relationships at each gauge location are essentially linear (e.g., Specimens D21-20, D21-25, D28-20 and D28-25). As the load increases, it is transferred to the interior of the CFRP laminate. The strains increase until debonding occurs. We observe that the strains rapidly change before CFRP laminate debonding. It can be concluded that it is appropriate to assume an effective bond length of about 200mm.

(a) D21-20 (b) D28-20 (c) D21-25 (d) D28-25

Figure 4. Failure modes of specimens in shear tests.

Table 4. Results of shear tests.

Specimens	Bond Length (mm)	Cracking Load (kN)	Ultimate Load (kN)	Effective Bond Length (mm)	Average Bond Stress (MPa)	Slip (mm)
D21-10	100	12.5	12.5	-	2.50	0.73
D21-15	150	15.5	15.5	-	2.07	0.96
D21-20	200	18.5	18.5	204	1.85	1.41
D21-25	250	19.0	22.5	204	1.86	1.45
D28-10	100	15.0	15.0	-	3.00	0.81
D28-15	150	18.5	18.5	-	2.47	1.13
D28-20	200	19.5	19.5	196	1.99	1.72
D28-25	250	20.0	21.5	196	2.04	1.61

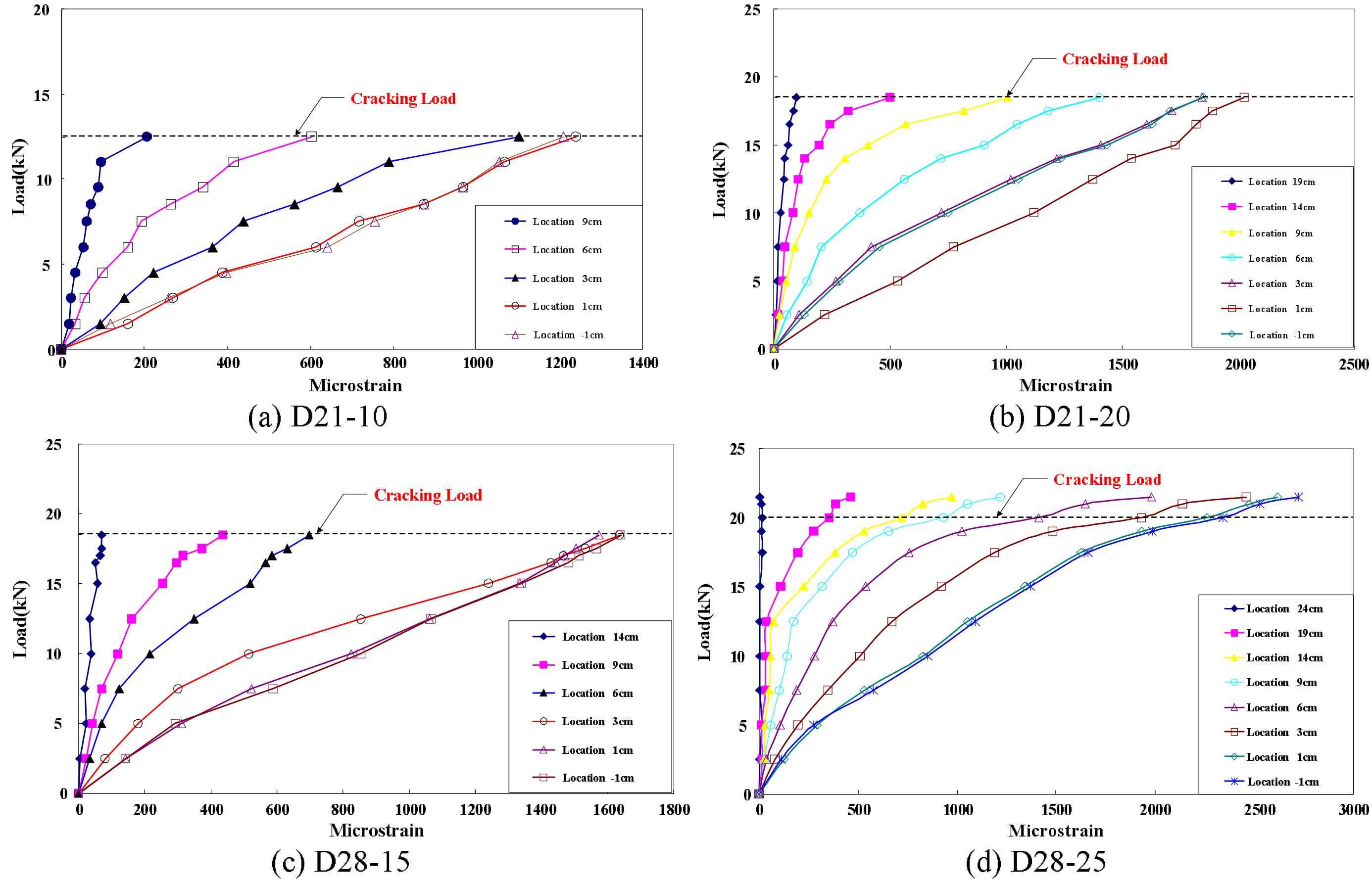

Figure 5. Load–CFRP strain curves at various gauge locations.

3.3 *Calculation of Bond Stresses and Slips*

The basic Equation relating bond stress and slip is developed in the following. We consider the basic interface between the CFRP laminate and concrete shown in Figure. 6(a).

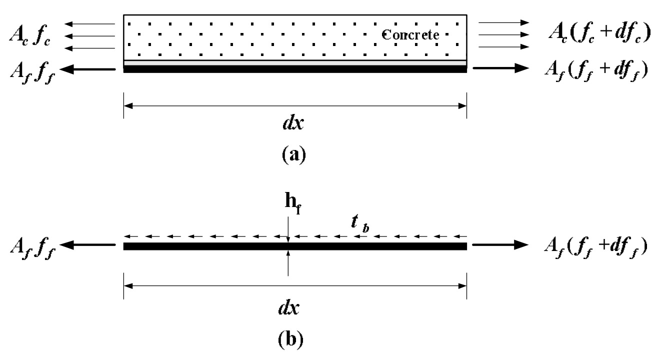

Figure 6. Bond stress between concrete and CFRP laminate.

The relation between the tensile load $A_f f_f$ and bond stress τ_b for an element of length dx is obtained from the equilibrium of the element shown in Figure. 6(b). This gives

$$A_c\, df_c + A_f\, df_f = 0 \tag{1}$$

$$\tau_b\left(b_f\, dx\right) = A_f\left(f_f + df_f\right) - A_f\, f_f \tag{2}$$

Rearranging these equations provides the following expression for the bond stress:

$$\tau_b = h_f \frac{df_f}{dx} = h_f E_f \frac{d\varepsilon_f}{dx} \tag{3}$$

The strain distribution curve of for the CFRP laminate is approximated by a quadratic curve from the measured CFRP laminate strains. If three data points $(x_{i-1}, \varepsilon_{i-1})$, (x_i, ε_i), $(x_{i+1}, \varepsilon_{i+1})$ are available, this leads to a second-order equation of the form

$$\varepsilon_s = \varepsilon(x) = a_i + b_i x + c_i x^2 \tag{4}$$

Three data points $(x_{i-1}, \varepsilon_{i-1})$, (x_i, ε_i), $(x_{i+1}, \varepsilon_{i+1})$ can be substituted into Equation. (4) to determine the coefficients a_i, b_i, c_i. From Equation. (3) and (4) we obtain the following relation to calculate the bond stress

$\tau_{bi}(x)$:

$$\tau_{bi}(x) = E_f\, h_f\left(b_i + 2c_i x\right) \tag{5}$$

The slip δ can be determined from the following equation:

$$\delta_i(x) = \delta_{i-1}(x) + \int_{x_{i-1}}^{x_i}\left(a_i + b_i x + c_i x^2\right)dx \tag{6}$$

The bond stress distributions and bond stress–slip results are plotted in Figure. 7 for those specimens having a bond length of 200mm and greater. The maximum calculated bond stresses are about 3.0~3.3MPa. The corresponding slips for the specimens having a 200mm bond length are about 0.3~0.42mm, while the slips for the 250mm bond length are about 0.8~1.1mm.

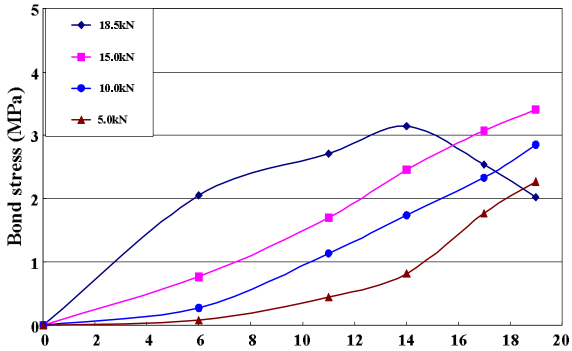

(a) Bond stress distribution of D21-20

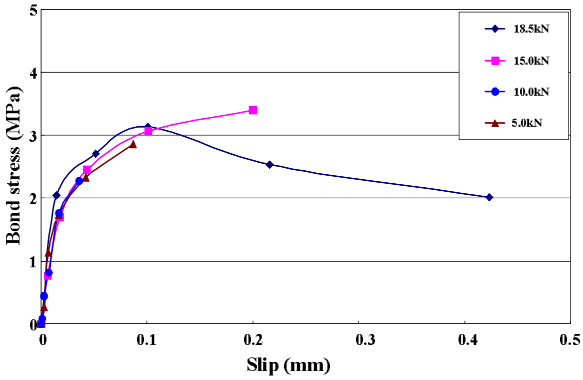

(b) Bond stress and slip of D21-20

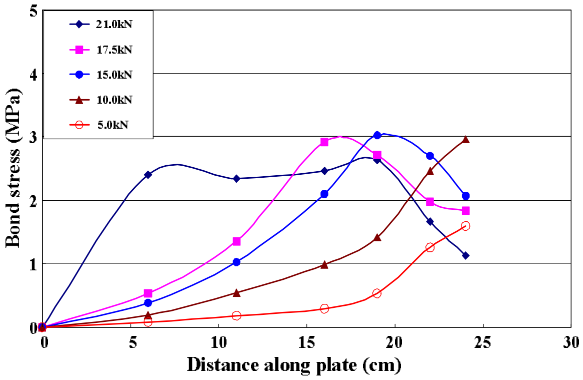

(c) Bond stress distribution of D21-25

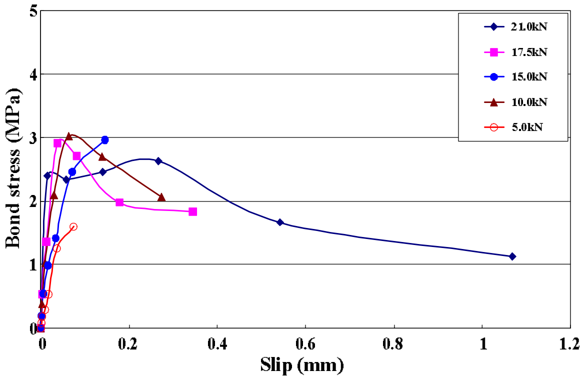

(d) Bond stress and slip of D21-25

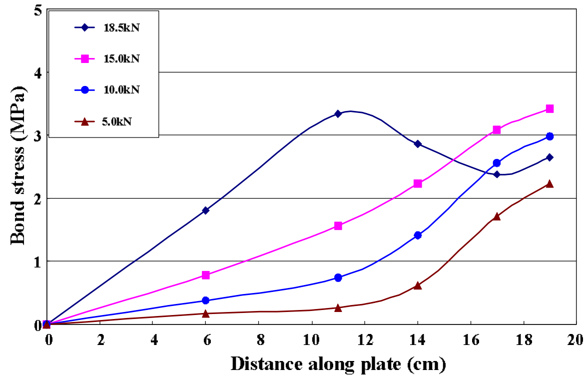

(e) Bond stress distribution of D28-20

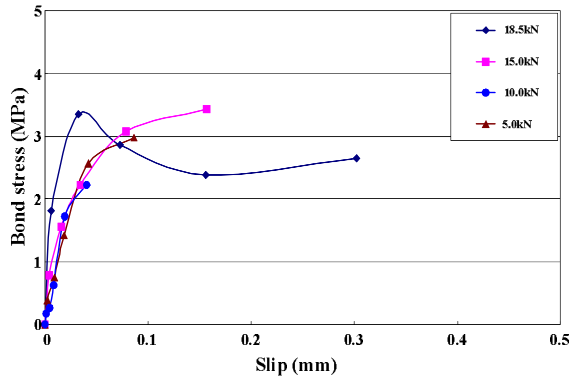

(f) Bond stress and slip of D28-20

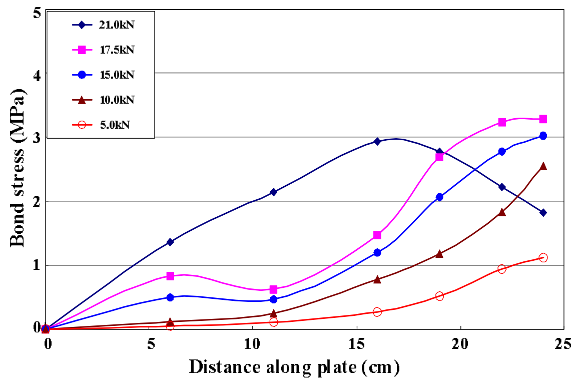

(g) Bond stress distribution of D28-25

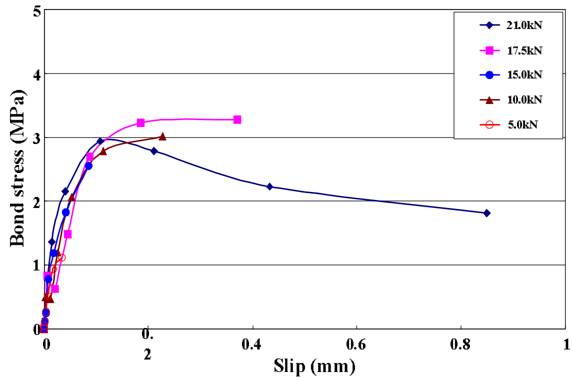

(h) Bond stress and slip of D28-25

Figure 7. Bond stresses and slips in shear tests.

3.4 *Approximate interfacial bond–slip model*

The bond–slip model for the interface between the CFRP laminates and the concrete, which governs debonding failures, has been estimated from the shear tests. In typical FRP-strengthened structures the bond length is generally greater than the effective bond length. Consequently, only those specimens having bond lengths greater than the effective bond length have been considered (i.e., Specimens D21-20, D21-25, D28-20 and D28-25).

The approximate bond–slip model is depicted in Figure. 8.

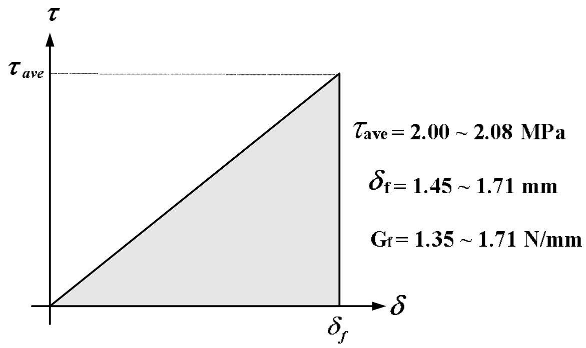

Figure 8. Approximate interfacial bond–slip model.

The important factors in this model are the average maximum bond stress and the corresponding amount of slip. The average maximum bond stresses are given in Table 4, while the amounts of slip have been determined from the relative slips between the concrete and CFRP laminates. As indicated in Figure. 8, the maximum average bond stresses were about 1.86~2.04MPa and the slip amounts between the CFRP laminates and concrete were in the range of 1.45~1.72mm. This gives an interfacial fracture energy (area under the $\tau - \delta$ curve) of about 1.35~1.71N/mm.

4 VERIFICATION FOR CFRP-STRENGTHENED RC BEAMS

4.1 *Beams*

Altogether five beams were tested in flexure. The beam geometry used was a rectangular section of 200mm(b)×300mm(h), as shown in Figure. 9.

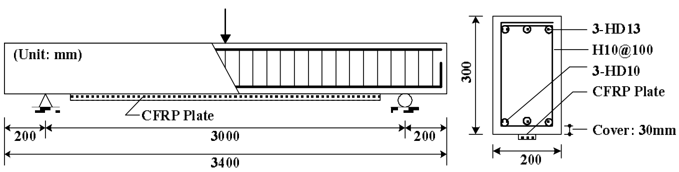

Figure 9. Geometry of CFRP-strengthened RC beams.

The specific beam designations and test variables are provided in Table 5.

All beams were reinforced with three D13 bars (diameter of 13mm) in the compression zone and three D10 bars (diameter of 10mm) in the tension zone. The beams were reinforced in shear with 10mm diameter stirrups spaced at 100 mm (Fig. 9). All the beam specimens were sufficiently designed to prevent shear failures.

Table 5.Details of beams in flexural tests.

Beams	CFRP Laminate			Remarks
	Layer	Width (mm)	Bond Length (mm)	
SBC	-	-	-	No strengthening
SBF1-B1	1	50	1800	1 laminate
SBF1-B2			2700	1 laminate
SBW2-B1		100	1800	2 laminates
SBW2-B2			2700	2 laminates

4.2 *Materials*

The type of concrete in the flexural tests was a ready-mixed concrete that had been aged for 28 days. Its specified concrete strength was 24.0MPa; its measured compressive strength was 20.7MPa and its slump value was 120mm. The design yield stresses of the 10mm and 13mm diameter reinforcing bars were 475.2MPa and 466.2MPa, respectively. The material properties of the CFRP laminates used for the flexural tests are as given in Table 1.

4.3 *Finite Element Analysis*

The finite element analysis of the experimentally tested CFRP-plated concrete beams was conducted using the DIANA software program. As shown in Figure. 10, the commonly used traditional plasticity representation is employed for the concrete in compression; the tensile behaviour consists of a smeared crack model, assuming micro-cracking. The steel reinforcing bars have an elasto-plastic linear hardening behaviour, with a typical modulus of elasticity of 200GPa. The interfacial behaviour between the CFRP laminates and the concrete is characterized using the approximate bond–slip model of Fig. 8, with the values obtained from the shear tests. The finite element model is a two-dimensional analysis, as shown in Figure. 11. Any bond–slip between the concrete and steel rebars is neglected in this analysis

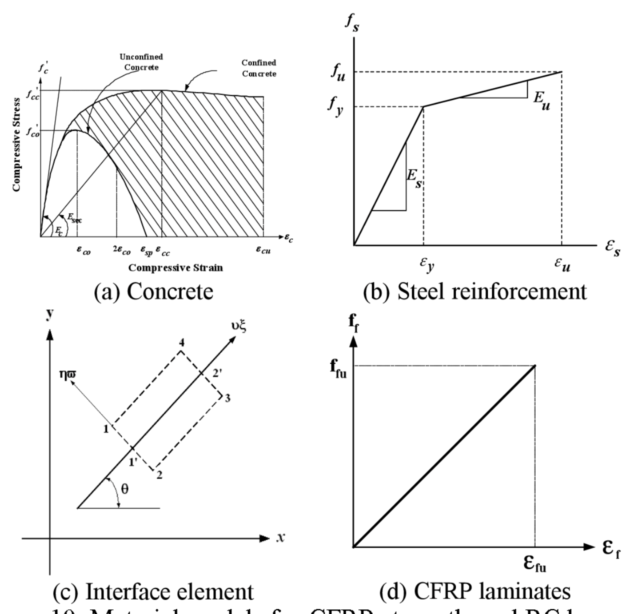

Figure 10. Material models for CFRP-strengthened RC beams.

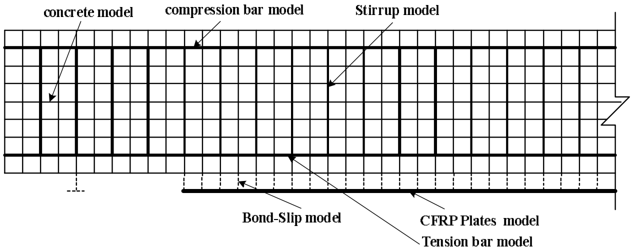

Figure 11. Finite element model of CFRP-strengthened RC beams.

4.4 *Results*

The four beams strengthened with bonded CFRP laminates and the control (un-strengthened) beam were subjected to flexural tests, and also analyzed using the above nonlinear finite element model. A comparison of the test results with the numerical predictions is given in Table 6. Figure 12 shows the experimental and numerical load–deflection relationships for the various specimens. Here it can be seen that the beams strengthened with 1 laminate of CFRP (50mm in width) had capacities that were 30~40% higher than that of the control beam; the capacities of the beams strengthened with two laminates in the width direction (100mm total width) were 70% or higher than that of the control beam.

The experiment and finite element simulation of the control beam yielded almost identical results. For the beams strengthened with CFRP laminates there were about 5~10% differences between the stiffnesses from the tests and numerical predictions. Also, for the beams strengthened with 1 and 2 CFRP laminates the deflections at debonding obtained from the analysis and the experiments were almost identical. As can be observed in Table 6, the average ratio of the test to the predicted value of the yield load is 0.95, with a coefficient of variation of 3.89%. For the debonding load, the average predicted to experimental ratio is 0.99, with a coefficient of variation of 3.59%. Thus, the proposed finite element analysis for CFRP-strengthened reinforced concrete beams, based on the bond–slip model at the interface between the concrete and CFRP laminates obtained from the shear tests, shows an excellent agreement with experimental results in terms of the yield and debonding loads.

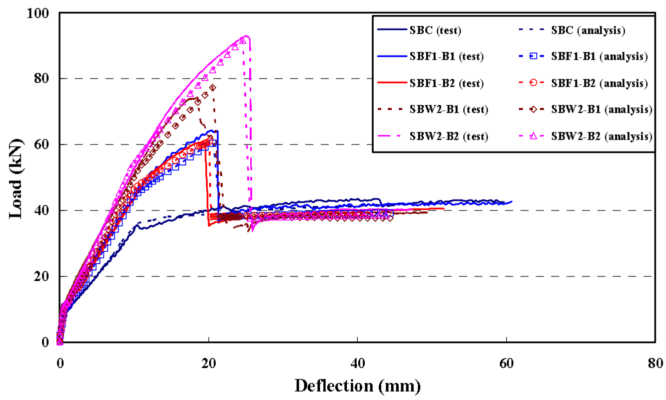

Figure 12. Experimental and numerical load–deflection curves for CFRP-strengthened beams.

Table 6. Experimental and numerical results for CFRP-strengthened beams.

Beams	Yield load			Debonding load			Failure
	Test (a) (kN)	Analysis (b) (kN)	(b)/(a)	Test (c) (kN)	Analysis (d) (kN)	(d)/(c)	
SBC	35.5	36.0	1.01	-	-	-	Flexural
SBF1-B1	47.2	44.1	0.93	64.2	60.4	0.94	Debonding
SBF1-B2	49.0	46.3	0.94	60.5	60.9	1.01	Debonding
SBW2-B1	60.4	54.7	0.91	74.3	77.2	1.04	Debonding
SBW2-B2	61.9	57.4	0.93	92.9	91.6	0.99	Debonding
Mean			0.95			0.99	
Coefficient of Variation (%)			3.89			3.59	

4.5 *Ductility*

Ductility is a qualitative concept representing inelastic deformational capacity of materials, sections, members or structures before they collapse. Ductility may be a very important safety factor that delays local failure by redistributing redundant stresses in the critical section of a statically indeterminate structure. A ductility index or ductility factor is used to quantify ductility. It is defined as ratios in terms of curvature, rotation and deflection. In this study, the ductility index is defined as the ratio of the deflection when the member is subject to the ultimate load (i.e., debonding load) to that when it yields. The ductility index for each beam is given in Table 7.

The ductilities of the CFRP-strengthened beams are greatly reduced compared to that for the control beam. The ductility indices in these beams are all less than 3.0 due to the brittle nature of the debonding failure modes. The average ratio of the test and predicted deflection values at the yield and debonding loads are 0.93 and 1.04, with coefficients of variation of 5.12% and 4.62%, respectively. Thus, the numerical analysis results of the reinforced concrete beams strengthened with CFRP laminates, which incorporates the proposed interfacial bond–slip model, shows a very good agreement with the experimental results in terms of the deflections at the debonding and yield loads.

5 CONCLUSIONS

In this investigation, shear tests were performed on specimens having CFRP laminates bonded to concrete

Table 7. Ductility indices for CFRP-strengthened beams.

Beams	Deflection of yield load			Deflection of debonding load			Ductility index	
	Test (a) (mm)	Analysis (b) (mm)	(b)/(a)	Test (c) (mm)	Analysis (d) (mm)	(d)/(c)	Test	Analysis
SBC	10.4	10.5	1.01	-	-	-	-	-
SBF1-B1	10.7	10.0	0.93	20.4	20.6	1.01	1.91	2.06
SBF1-B2	11.5	10.0	0.87	18.9	20.1	1.06	1.64	2.01
SBW2-B1	12.4	11.5	0.93	18.5	20.5	1.11	1.49	1.78
SBW2-B2	12.3	11.0	0.89	24.9	24.5	0.98	2.02	2.23
Mean			0.93			1.04		
Coefficient of Variation (%)			5.12			4.62		

prisms. Two concrete compressive strengths and various bonding lengths were considered. The effective bond lengths and an approximate interfacial bond-slip model were estimated for each concrete compressive strengths.

In addition, flexural tests and a finite element analysis with the interfacial bond–slip model incorporated in the DIANA software program were performed for CFRP-strengthened reinforced concrete beams. The findings of the study can be summarized as follows:

1) The bond–slip model for the interface between the CFRP laminates and concrete, which governs debonding failures, was estimated from the double-shear tests having as parameters bond length and concrete compressive strength. The average maximum bond stress and effective bond length for the specimens were calculated using a linear regression analysis.

2) The finite element analysis of reinforced concrete beams strengthened with externally bonded CFRP laminates was carried out using the DIANA program; the nonlinear material models in that software for the concrete and steel reinforcement, and the interfacial bond–slip model between the concrete and CFRP laminates from the shear test, were employed.

3) Flexural tests were performed on reinforced concrete beams strengthened with CFRP laminates. From the flexural test results, it was seen that the beams strengthened with 1 laminate (50mm in width) had capacities 30~40% higher than that of the control beam, and the beams strengthened with 2 laminates in the width direction (100mm total width) had 70% or higher load capacities than that of the control beam.

4) It has been verified that, for reinforced concrete beams strengthened with externally bonded CFRP laminates, the nonlinear finite element analysis based on the proposed interfacial bond–slip model gives very good agreement with experiment results in terms of the debonding loads, yield loads, and ductility.

REFERENCES

Alfarabi SA, Al-Sulaaimani GJ, Basunbul IA. Strengthening of initially loaded reinforced concrete beams using FRP plates. ACI Structural Journal 1994; 91:160–168.

Arduini M, Tommaso A, Nanni A. Brittle failure in FRP plate and sheet bonded beams. ACI Structural Journal 1997; 94(4):363–370.

Bizindavyi L, Neale KW. Transfer lengths and bond strengths for composites bonded to concrete. Journal of Composites for Construction, ASCE 1999; 3(4):153–160.

Brosens K, Gemert D. Anchoring stresses between concrete and carbon fibre reinforced laminates. In: Proceedings of the Third International Symposium on Non-metallic (FRP) Reinforcements for Concrete Structures. 1997.

Chen JF, Teng JG. Anchorage strength models for FRP and Steel plates boned to concrete. Journal of Structural Engineering 2001; 127(7):784–791.

Fanning PJ, Kelly O. Ultimate response of RC beams strengthened with CFRP plates. Journal of Composites for Construction, ASCE 2001; 5(2):122–127.

KICT. Development of New Technology on Strengthening RC Structures with Externally Post-tensioning CFRP Strips (1st Year). In: Report of Korea Institute of Construction Technology 2004, In Korean.

Malek AM, Saadatmanesh H, Ehsani MR. Prediction of failure load of R/C beams strengthened with FRP plate due to stress concentration at the plate end. ACI Structural Journal 1998; 95(1):142–152.

Mander JB, Priestley MJ, Park R. Theoretical stress-strain model for confined concrete. Journal of Structural Engineering, ASCE 1998; 114(8):1804–1849.

Michel J, Chajes TF, Januszka DR, Mertz TA, Thomson JR, Willam WF. Shear strengthening of reinforced concrete beams using externally applied composite fabrics. ACI Structural Journal 1995; 295–303.

Mukhopadhyaya P, Swamy RN. Interface shear stress: a new design criterion for plate debonding. Journal of Composites for Construction, ASCE 2001; 5(1):35–43.

Naaman AE, Alkhairi FM. Stress at ultimate in unbonded post-tensioning tendon: part 2-Proposed Methodology. ACI Structural Journal 1991; 88(6):683–690.

Oehlers DJ. Reinforced concrete beams with plates glued to their soffits. Journal of Structural Engineering, ASCE 1992;118(8):2023–38.

Park SK, and Yang DS. Flexural behavior of reinforced concrete beams with cementitious repair materials. Materials and Structures 2005; 38:329–334.

Rahimi H, Hutchinson A. Concrete beams strengthened with externally bonded FRP plates. Journal of Composites for Construction, ASCE 2001; 5(1):44–56.

Smith ST, Teng JG. FRP-strengthening RC beams, II: assessment of debonding strength models. Engineering Structures 2002; 24:397–417.

Smith ST, Teng JG. Shear-bending interaction in debonding failures of FRP-plated RC beams. Advanced Structure Engineering 2003; 6(3):183–200.

Teng JG, Smith ST, Yao J, Chen Jf. Intermediate crack-induced debonding in RC beams and slabs. Construction and Building Materials 2003; 447–462.

Ziraba YN, Baluch MH, Basunbul AM, Sharif IA, Azad AK, Al-Sulaimani GJ. Guidelines towards the design of reinforced concrete beams with external plates. ACI structural Journal 1994; 91(6):639–646.